Am J Transl Res 2024;16(11):7036-7053
www.ajtr.org /ISSN:1943-8141/AJTR0159017

Original Article

Cistanche deserticola polysaccharide alleviates constipation by regulating intestinal barrier function and intestinal microbiota and their metabolites

Ziqing Yu[1*], Zhaopeng Zhang[2*], Chunjie Hu[3], Lulu Xie[3], Ru Zhang[1], Rui Gao[1], Zhirun Zhang[1], Xuyang Wei[1], Ting Li[3], Junpeng Guo[1]

[1]*School of Clinical Medicine, Changchun University of Chinese Medicine, Changchun 130117, Jilin, China;* [2]*School of Pharmacy, Changchun University of Chinese Medicine, Changchun 130117, Jilin, China;* [3]*College of Traditional Chinese Medicine, Changchun University of Chinese Medicine, Changchun 130117, Jilin, China.* [*]*Equal contributors and co-first authors.*

Received July 6, 2024; Accepted October 29, 2024; Epub November 15, 2024; Published November 30, 2024

Abstract: Constipation is a clinical condition characterized by reduced intestinal motility, dry and hardened stool, and prolonged retention. Common constipation medicines are less stable, and prolonged use can lead to dependency and side effects. *Cistanche deserticola Ma,* a well-known Traditional Chinese Medicine, is frequently used to alleviate constipation. In this study, we established a loperamide-induced constipation model in mice to investigate the effects of *Cistanche polysaccharide*s (CDPS) and to explore its underlying pharmacological mechanism. The serum levels of inflammatory factors, gastrointestinal hormones and neurotransmitters of mice were measured by enzyme-linked immunosorbent assay (ELISA). Intestinal tight junction integrity was evaluated using immunohistochemistry, and Western blot was used to detect tight junction protein levels. Gut microbial community structure and metabolite content were determined using 16S rRNA sequencing and metabolomics analysis. Oral CDPS enhanced the intestinal tight junction integrity, improved barrier function of intestinal mucosa, reduced inflammation, restored intestinal microbiota balance, and regulated metabolite levels. Notably, CDPS increased the abundance of beneficial bacteria, including *Prevotellaceae UCG-001*, *Odoribacter*, *Clostridiales vadin BB60* group, *Alistipes*, *Lactobacillaceae*, and *Rikenellaceae*, while decreasing the abundance of harmful bacteria such as *Parabacteroides* and Proteobacteria. In summary, CDPS may prevent and treat constipation by modulating intestinal flora composition, influencing metabolite profiles, and reinforcing mucosal barrier function.

Keywords: Constipation, *Cistanche deserticola* polysaccharide, tight junction, faecal microbiome, intestinal inflammation

Introduction

Constipation is a clinical condition characterized by reduced intestinal motility, dry and hardened stool, and prolonged retention [1]. Constipation affects over 15% of the global population, rendering it one of the most prevalent intestinal disorders [2]. Current treatments for constipation include surgical or medical approaches with common clinical therapeutic agents, such as prokinetic agents, secretagogues, and laxatives [3, 4]. While these drugs can be effective, they often lack stability, leading to high patient dependency, drug tolerance and adverse reactions with a long-term use [5, 6]. Therefore, finding a drug or clinical treatment with stable efficacy and high safety is crucial for improving treatment outcomes.

Understanding the biology of the human gut microbiome has enabled a systematic exploration of how gut microbiota affects the human body [7]. A balanced gut microbiome is crucial in upholding the functional homeostasis of the host's metabolic, immune, digestive, and developmental systems [8, 9]. Diseases disrupt the gut microbiome environment, reducing beneficial bacteria populations and promoting harmful bacteria, which impairs the body's homeostatic regulation. Constipation primarily affects

https://doi.org/10.62347/RQBJ2018

the colorectum, with its integrity directly affected by the changes in the intestinal flora. Factors such as endocrine dysfunction, altered intestinal hormones, and disordered water and sodium transport exacerbate constipation development [10, 11]. Therefore, drugs that can restore gut microbiota structure and strengthen gut barrier function are promising options for treating constipation [12, 13].

Traditional Chinese Medicine (TCM) is known for its ability to improve digestion and relieve constipation with a favorable safety profile, making it a focal point for research and development in this field. *Cistanche* is a traditional Chinese herbal medicine believed to warm the kidneys, promote bowel movements, regulate endocrine system, and protect neural function [14, 15]. One of its active ingredients is *Cistanche polysaccharide* (CDPS), which has been reported to regulate the structure of intestinal microbiota, optimize the intestinal environment, regulate the concentration of neurotransmitters, and alleviate constipation [16-19]. While CDPS has demonstrated efficacy in alleviating constipation, its potential pharmacological mechanisms remain unclear.

In this study, we demonstrated the efficacy of CDPS in relieving constipation symptoms in a mouse model and explored its pharmacological mechanisms using multi-omics analysis. Our findings provide a theoretical basis for the clinical use of CDPS in treating constipation, potentially benefiting a broader range of constipation patients.

Materials and methods

Materials and reagents

The polysaccharide in *Cistanche deserticola Ma* (CDPS) was obtained from Chengdu Aifa Biotechnology Co., Ltd. (Sichuan, China). Loperamide (LOP) capsules (2 mg/capsule) were purchased from Xi'an Janssen Pharmaceutical Ltd. (Shanxi, China). Mosapride (MOS) citrate dispersible tablets were obtained from Chengdu Kanghong Pharmaceutical Group Co., (Sichuan, China). Acetonitrile, formic acid, and methanol in HPLC grade were purchased from Fisher Company (Shanghai, China), and HPLC-grade L-2-chlorophenylalanine was obtained from Hengchuang Biotechnology Co., Ltd. (Shanghai, China). Enzyme-linked immunosorbent assay (ELISA) kits for IL-6, IL-1β, TNF-α, somatostatin (SS), serotonin (5-HT), and motilin (MTL) were purchased from Beijing Huaying Biotechnology (Beijing, China).

Animals and treatments

The study adhered to ARRIVE guidelines [20], with experimental procedures approved by Changchun University of Chinese Medicine and the Institutional Animal Care Committee (Approval No. 2023548). Forty 6-week-old C57BL/6 male mice (20 ± 2 g) were sourced from Liaoning Changsheng Biotechnology Co., Ltd. (Liaoning, China). The mice were fed in a standard environment at 25 ± 2°C room temperature, 50% ± 5% humidity, and a 12-h light-dark cycle. After 1 week of acclimation, the mice were randomly assigned to 4 groups (n = 10): Control (Control), Model (only LOP), MOS (LOP+MOS), and CDPS (LOP+CDPS) groups. The control group was given an equal volume of normal saline, while the mouse constipation model was induced in the other groups based on previous studies [21], with each mouse (except for control group) receiving an oral dose of 10 mg/kg LOP once daily for two weeks. After modelling, one mouse was dissected to confirm successful modeling by observing stool accumulation in the colon (spherical or beaded stools with no residue in the jejunum and ileum). The experimental design and protocol of mouse dosing are shown in **Figure 1A**. During the treatment period, LOP administration continued at the same dosage. In the meantime, 3 mg/kg MOS was given to the MOS group and the CDPS group was treated using 100 mg/kg CDPS, all drugs were orally administered once daily for 2 weeks. The LOP dosage was referenced from literature [21], the MOS dosage was adjusted for mice based on instruction guidelines, and the CDPS dose was determined according to our preliminary experimental results.

Analysis of serum biochemical indices

Plasma was collected from the orbital venous plexus of each mouse. Plasma was centrifuged at 3500 rpm for 10 min (centrifugation radius of 5.5 mm) after 30 min of quiescence, and 100 μL of serum was collected into 1.5 mL EP tube. Then, the serum levels of IL-6, IL-1β, TNF-α, SS, 5-HT, and MTL in mice were detected using ELISA assay, following the manufacturers' instructions.

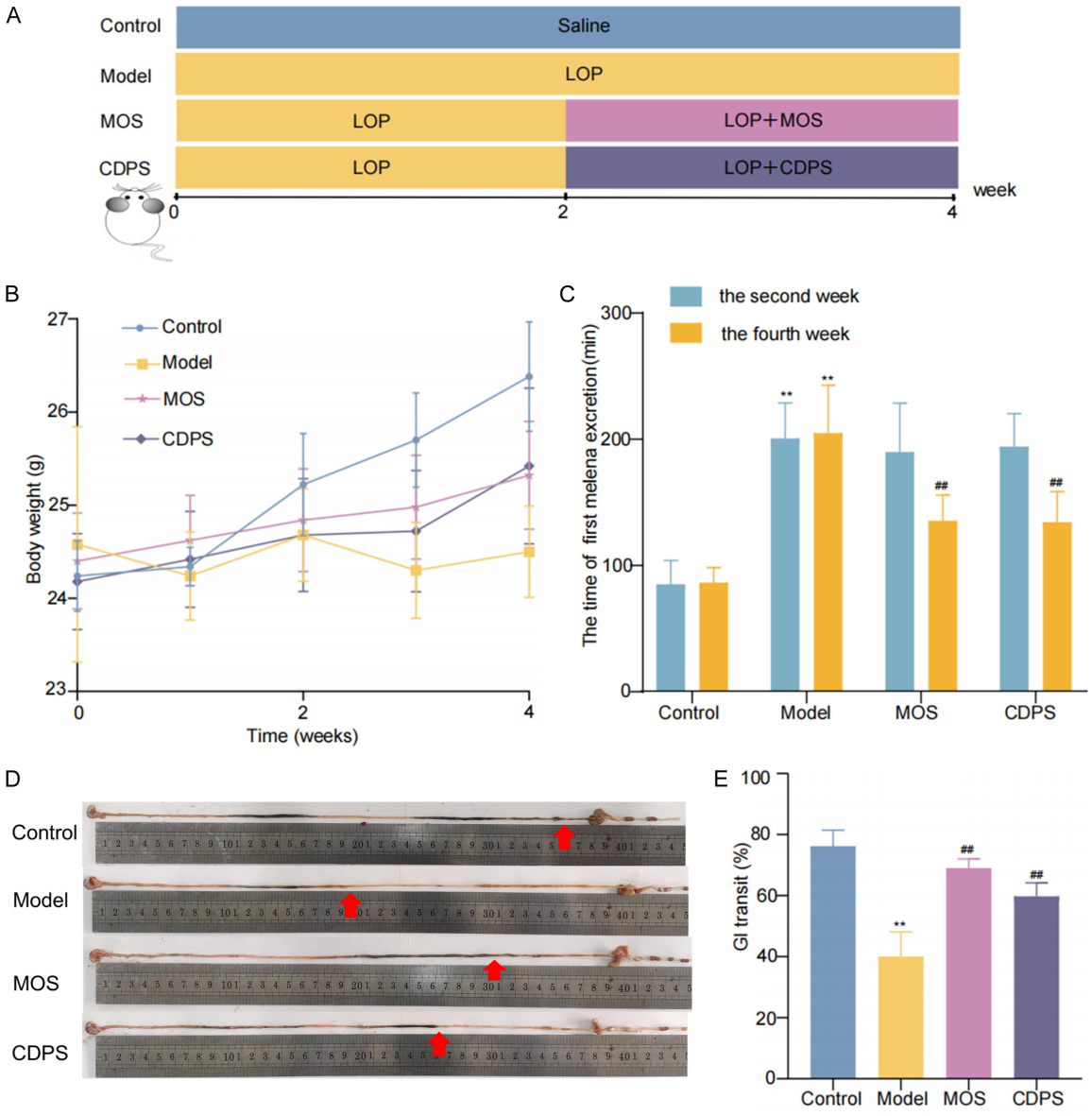

Figure 1. *Cistanche deserticola* polysaccharide (CDPS) improved the general physiological conditions and defecation-related parameters in constipated mice. A. Schematic diagram of the experimental interventions with CDPS in constipated mice. B. Body weight changes observed during the entire experiment. C. The time to first melena excretion. D. Propulsion distance of active charcoal meal in the small intestine. E. Gastrointestinal (GI) transit rates. Data are represented as mean ± SEM (n = 5). $^{**}P < 0.01$, compared with the Control group; $\#\#P < 0.01$, compared with the Model group.

Determination of gastrointestinal (GI) transport rate

The GI transport rate was measured based on previously established methods [22]. After treatment, all mice were fasted for 12 h, followed by oral administration of an activated charcoal suspension. The GI transit rate for each group was determined by assessing the proportion of the distance travelled by charcoal powder relative to the total length of the small intestine. GI transport rate (%) = propulsion distance of activated carbon turbidity from pylorus (cm)/total intestinal length (cm) × 100%.

Intestinal permeability test

Within 48 hours of completing the treatment, intestinal permeability in rats was indirectly determined by high-performance liquid chro-

matography (HPLC). A solution containing 50 mg of lactulose and 25 mg of mannitol was administered via slow gavage (1 mL per rat). Urine was collected within 8 hours and preserved with an appropriate amount of sulfosalicylic acid at -20°C. The concentrations of lactulose and mannitol in the urine were then determined by HPCL, and the excretion rate for each compound was calculated. Intestinal permeability was determined by calculating the lactulose-to-mannitol (L/M) excretion ratio.

Hematoxylin and eosin (H&E) staining

Ileal tissues were collected and fixed in a 4% paraformaldehyde solution, then dehydrated, embedded in paraffin, and sliced into 3-μm thick sections. Haematoxylin-eosin (H&E) staining was performed using an H&E staining kit for histomorphometric evaluation of the ileal tissues. The stained sections were imaged under a light microscope. To quantify infiltrated inflammatory cells and mucosal layer thickness, tissue sections were analyzed with H&E staining to highlight inflammatory cells. The percentage of inflammatory cells was determined by calculating their proportion relative to the total cell count in each observed field. Specifically, three random fields per section were analyzed under a high-power field (×400 magnification) using ImageJ 6.0 software. Inflammatory cells within both the mucosal and submucosal layers were counted to obtain an overall infiltration percentage. The thickness of the mucosal layer was measured under a microscope at ×200 magnification by selecting five random fields on each section. The thickness from the base of the mucosa to the tip of the villi was measured using ImageJ software.

Immunohistochemistry

Immunohistochemical (IHC) staining was performed on ileal tissue sections to measure the protein expression of OCLN and ZO-1. The sections were deparaffinized in an oven at 65°C for 15 min, soaked in different concentrations of ethanol and placed in antigen retrieval solution at high temperature for 10 min. After washing with PBS, the sections were incubated with 5% bovine albumin blocking solution for 60 minutes. Following another PBS rinse, the sections were incubated overnight at 4°C with primary antibodies: OCLN (1:400, Proteintech) and ZO-1 (1:400, Proteintech). On the following day, sections were treated with an HRP-labeled secondary antibody (goat anti-mouse) for 45 minutes. After a 20-second incubation with DAB (diaminobenzidine) diluent, the staining was promptly terminated with deionized water, and sections were counterstained with hematoxylin for 15 seconds. The stained sections were observed under an optical microscope, and protein expression levels were analyzed using ImageJ 6.0 software.

Western blot

Total protein was extracted from mouse intestinal tissue samples using RIPA buffer containing phosphatase inhibitors. Protein concentration in each sample was determined using a BCA protein assay kit. Sodium dodecyl sulphate-polyacrylamide gel electrophoresis (SDS-PAGE) was performed by loading 10 μL sample to each well. Electrophoresis was conducted at 80 V for 20 minutes through the stacking gel, followed by 120 V for 90 minutes through the separating gel. Proteins were then transferred to a polyvinylidene fluoride (PVDF) membrane using wet transfer with 10% SDS polyacrylamide gel. The membranes were blocked in 10% fetal bovine serum for 2 h at room temperature, and then incubated overnight at 4°C with primary antibodies: β-actin (1:5000, Proteintech), OCLN (1:10000, Proteintech), ERK (1:8000, Proteintech), p-ERK (1:4500, Cell Signaling), P38 (1:6000, Proteintech), and p-P38 (1:2000, Proteintech). The membranes were washed 3× with TBST buffer and incubated with secondary antibodies at room temperature. Finally, the protein bands were visualized with a chemiluminescence imaging system.

Microbiome analysis

Genomic DNA was extracted from samples using a MagPure Soil DNA LQ Kit (Magen, China), following the manufacturer's instructions. The extracted DNA was stored at -20°C until use. For bacterial 16S rRNA gene amplification, specific barcoded primers and a Takara Ex Taq high-fidelity enzyme were used. The hypervariable regions (V3-V4) of 16S rRNA gene were amplified using the universal primers: 343 F (5'-TACGGRAGGCAGCAG-3', where 'R' denotes a purine, either guanine (G) or adenine (A)) and 798 R (Reverse, 5'-AGGGTATCTAATCCT-3') to assess bacterial diversity. The products were purified with AMPure XP mag-

netic beads and amplified by a 2-round PCR. The PCR products were purified using magnetic beads and quantified with a Qubit fluorometer. Product concentrations were adjusted for sequencing, and the constructed libraries were sequenced on an Illumina NovaSeq 6000 platform. The sequencing data was analyzed through Ouyi cloud platform (https://cloud.oebiotech.com), provided by Shanghai Ouyi Biomedical Biotechnology Co., Ltd. (Shanghai, China).

Metabolomic analysis

Fecal samples were initially stored at -80°C and thawed at room temperature prior to processing. Subsequently, 400 μL of a protein-precipitating methanol-acetonitrile mixture was added to the samples. The mixture was sonicated for 10 min in an ice-water bath and allowed to stand at -40°C for 30 min. The mixture was centrifuged for 10 min, and 150 μL of the supernatant was aspirated and filtered through a 0.22 μm organic phase pinhole filter. Quality control samples were prepared by pooling equal volumes of extracts from all samples. Liquid chromatography-mass spectrometry was performed using an ACQUITY UPLC I-Class PLUS spectrometer (Waters Corporation), and the mass spectrometry conditions are shown in Table S1. The chromatographic separation was performed on an ACQUITY UPLC HSS T3 column (100 mm × 2.1 mm, 1.8 um), with 0.35 mL/min flow rate and 2 uL injection volume, set at 45°C using mobile phases A (0.1% formic acid in water) and B (acetonitrile), and the gradient elution programs are shown in Table S2. Mass spectra were collected by scanning in positive and negative ion modes. Bioinformatic analysis was performed on the Ouyi cloud platform (https://cloud.oebiotech.com).

Statistical analysis

Data were presented as mean ± SEM (standard error of the mean) and visualized using GraphPad Prism 8.0.2 (GraphPad Software, La Jolla, CA, USA). Statistical analyses were conducted using IBM SPSS Statistics 27.0 (IBM Corporation, Armonk, NY, USA). For comparisons between two groups, an unpaired t-test was used, while an one-way analysis of variance (ANOVA) followed by Tukey's post hoc test was employed for comparisons among four groups. Statistical significance was defined as $P < 0.05$.

Results

CDPS ameliorated constipation in mice

LOP was used to induce the mouse constipation model, followed by CDPS treatment. Results showed that compared to the control group, the body weight of the mice in model group significantly decreased, and the time to the first black stool excretion was significantly increased. After CDPS treatment, body weight of mice increased and the time to the first black stool excretion was shortened (**Figure 1B**, **1C**). In addition, intestinal transit rate was significantly decreased in constipated mice, but improved after CDPS treatment (**Figure 1D**, **1E**). These findings were consistent with a positive control drug, MOS, indicating that CDPS can ameliorate constipation by enhancing gastrointestinal motility and accelerating GI transit.

Effect of CDPS on serum biochemical and histological parameters in constipated mice

Histopathological and serum biochemical analyses were performed on the small intestine tissues of mice with LOP-induced constipation to investigate the therapeutic effect of CDPS. Constipation causes pathomorphological changes, such as thinning of the small intestinal tissue and intestinal wall, intestinal mucosal damage, and rupture and incompleteness of intestinal villi in mice [23, 24]. Mice in the Model group exhibited damaged villi and local inflammatory cell infiltration in the small intestine compared to the Control group (**Figure 2A**). Following CDPS treatment, inflammatory cell infiltration in the mucosal and submucosal layers decreased, and mucosal integrity improved (**Figure 2B**, **2C**). ELISA results showed that compared with the control group, expression levels of MTL and 5-HT were decreased in the Model group, while SS expression levels were significantly increased. Conversely, CDPS treatment caused a substantial rise in MTL and 5-HT levels and a drop in SS levels (**Figure 2D-F**); these neurotransmitters are pivotal in modulating gastrointestinal motility [25]. In addition, serum levels of the inflammatory cytokines IL-6, IL-1β, and TNF-α were elevated in

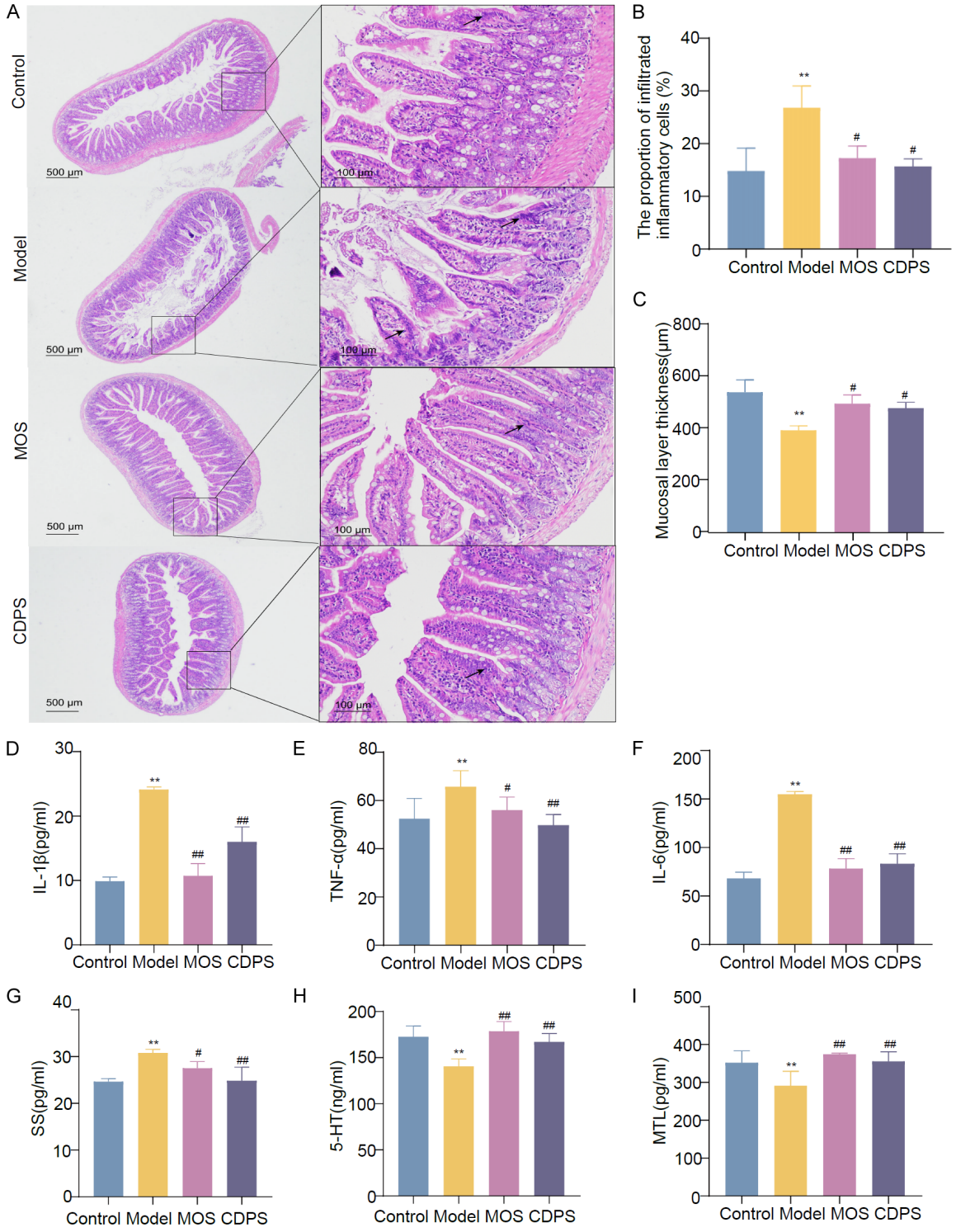

Figure 2. Effect of *Cistanche deserticola* polysaccharide (CDPS) on serum inflammatory factors, neurotransmitter levels, gastrointestinal hormones, and small intestine histology in constipated mice. A. Histopathologic features of the small intestine. Arrows indicate infiltrating inflammatory cells. B. The proportion of infiltrated inflammatory cells (n = 3). C. Mucosal layer thickness (n = 3). D. Mouse serum IL-1β levels. E. Mouse serum tumor necrosis factor alpha (TNF-α) levels. F. Mouse serum IL-6 levels. G. Mouse serum somatostatin (SS) levels. H. Mouse serum serotonin (5-HT) levels. I. Mouse serum motilin (MTL) levels. Data are represented as mean ± SEM. $^{**}P < 0.01$, compared with the Control group; $^{\#}P < 0.05$, $^{\#\#}P < 0.01$, compared with the Model group.

the Model group compared to the Control group. Nevertheless, CDPS treatment significantly reduced the levels of all 3 inflammatory factors (**Figure 2G-I**). These results demonstrate that CDPS has anti-inflammatory effects and improves constipation in LOP-induced model by modulating concentrations of gastrointestinal hormones and neurotransmitters.

CDPS regulated intestinal barrier function in constipated mice

We examined the expression of proteins that maintain the intestinal barrier function to explore whether the CDPS constipation-alleviating effects are associated with the intestinal barrier function. IHC staining was performed on small intestine tissue sections using antibodies for ZO-1 and OCLN, proteins essential for preserving the integrity of the gut mechanical barrier [26]. The expression levels of ZO-1 and OCLN were significantly decreased in the intestinal tissue of the Model group compared with the Control group. Conversely, the expression of both proteins significantly increased following CDPS treatment (**Figure 3A**, **3B**), which was confirmed through Western blotting (**Figure 3C**). Two isoforms of the MAPK signaling pathway, P38 and ERK, have been reported to play important roles in maintaining the intestinal barrier function and regulating intestinal inflammation [27]. Thus, we quantified the expression and phosphorylation levels of P38 and ERK in small intestinal tissues, and found that compared with the Model group, CDPS treatment effectively reduced p-P38 and p-ERK levels (**Figure 3D**, **3E**), suggesting that CDPS can inhibit P38 and ERK activation to enhance the structural integrity of the intestinal barrier.

CDPS restored gut microbiota structure in constipated mice

The homeostasis of gut microbiota is essential for safeguarding the integrity of the intestinal mucosal barrier, reducing inflammation, and enhancing gastrointestinal motility. We analyzed fecal samples of mice using 16S rRNA sequencing to investigate how CDPS influences the functional structure of the gut microbiota. The rarefaction curve reached a plateau (Figure S1), suggesting sufficient sequencing depth for detecting alpha diversity. Higher Chao1 index in the CDPS group than in the Model group indicated that CDPS treatment promoted a significant increase in species abundance (**Figure 4A**). Moreover, a principal coordinate analysis uncovered a clear separation in bacterial community structure between the Model and CDPS groups, suggesting substantial reorganization of the gut microbiota following CDPS treatment (**Figure 4B**). Thus, we examined the relative abundance of the top 20 bacteria at the phylum, family, and genus levels to characterize the effects of CDPS on gut microbiota composition. The phylum-level results showed that bacterial abundance was mainly concentrated in Firmicutes, Bacteroidetes, and Proteobacteria phyla (**Figure 4C**). Notably, a significant increase in the community abundance of Proteobacteria was detected, with the proportion rising to 15.2% ± 2.1% in the Model group compared to 8.5% ± 1.0% in the Control group. Nonetheless, CDPS treatment reduced the abundance of Proteobacteria in the CDPS group to 6.6% ± 1.4%. At the family level, significant changes were identified in the community abundance of *Rikenellaceae* and *Lactobacillaceae* (**Figure 4D**, **4E**). While the abundance of *Lactobacillaceae* decreased to 4.0% ± 0.9% in the Model group compared with 7.1% ± 2.5% in the Control group, it increased to 12.2% ± 4.9% in the CDPS group. *Lactobacillaceae* plays a crucial role in enhancing the function of the intestinal barrier, promoting beneficial bacteria, reducing harmful bacteria, decreasing intestinal inflammation and strengthening the intestinal barrier function [28, 29].

Characterization of gut microbiota in constipated mice

The association between CDPS treatment and gut microbiota was confirmed using Spearman rank analysis. A heatmap of top 20 genera, based on average abundance, revealed significant changes in the gut microbiota composition across experimental groups (**Figure 5A**). At the genus level, we observed strong associations between most bacteria and constipation-related indicators (**Figure 5B**). Notably, *Odoribacter* and *Alistipes* exhibited positive correlations with the GI transit rate and negative correlations with SS, IL-1β, and IL-6. Furthermore, *Clostridiales vadin BB60* group showed a positive correlation with 5-HT. The relative abundances of *Rikenellaceae*, *Odoribacter*, *Clostridiales vadin BB60* group, and *Alistipes* were significantly higher in the CDPS group than in the Model group, while *Parabacteroides* abun-

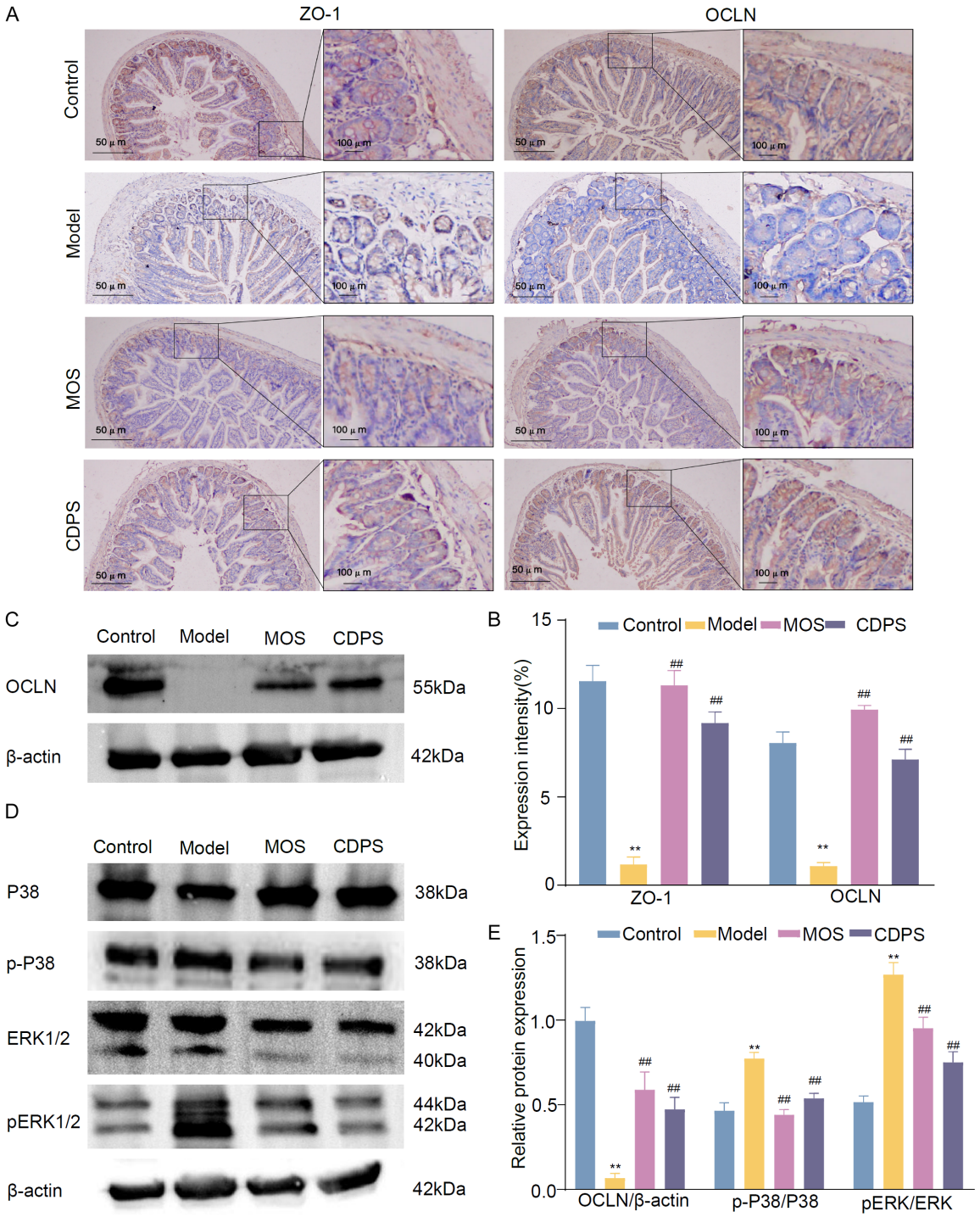

Figure 3. *Cistanche deserticola* polysaccharide (CDPS) regulated intestinal barrier function in constipated mice. (A) Immunohistochemical analysis of ZO-1 and OCLN proteins and (B) their expression intensity in small intestinal tissues. (C) OCLN/β-actin levels determined by Western blotting. (D) Levels of p-P38/P38 and p-ERK/ERK determined by Western blotting. (E) OCLN/β-actin, p-P38/P38, p-ERK/ERK protein expression levels. Data are represented as mean ± SEM (n = 3). $^{**}P < 0.01$, compared with the Control group; $^{\#\#}P < 0.01$, compared with the Model group.

dance was lower in the CDPS group (**Figure 5C-G**). *Odoribacter* effectively mitigates intestinal inflammation by increasing concentrations of SCFAs [30]. *Clostridiales vadin BB60* group from the *Clostridiaceae* family promotes intestinal peristalsis by stimulating the enterochro-

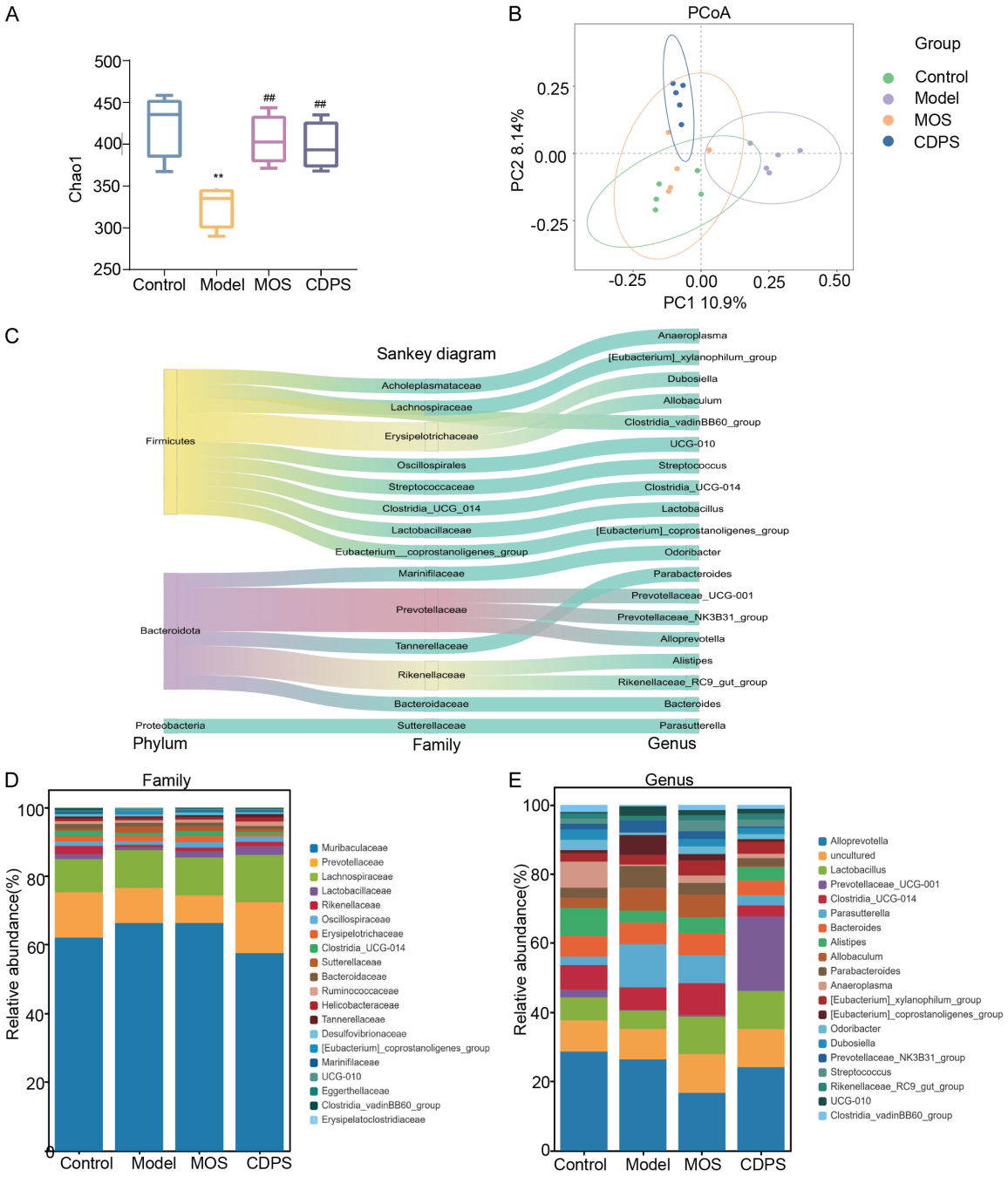

Figure 4. *Cistanche deserticola* polysaccharide (CDPS) restored gut microbiota structure in constipated mice. (A, B) Alpha diversity determined with Chao1 index (A), and beta diversity deduced using principal coordinate analysis (PCoA) (B). (C) Analysis of relative abundance of bacteria at phylum, family, and genus levels visualized as Sankey diagram. (D) Changes in top 20 gut microbiota at the family level. (E) Changes in top 20 gut microbiota at the genus level. Data are represented as mean ± SEM (n = 4). $^{**}P < 0.01$, compared with the Control group; $^{\#\#}P < 0.01$, compared with the Model group.

maffin cell biosynthesis and 5-HT release in the gut [31]. *Alistipes,* part of the *Rikenellaceae* family, shows an increased abundance in TRPA1 knockout mice, indicating a positive association between *Rikenellaceae* and intestinal peristalsis [32]. In addition, *Alistipes* and *Rikenellaceae* alleviate constipation by increasing butyric acid production and promoting the

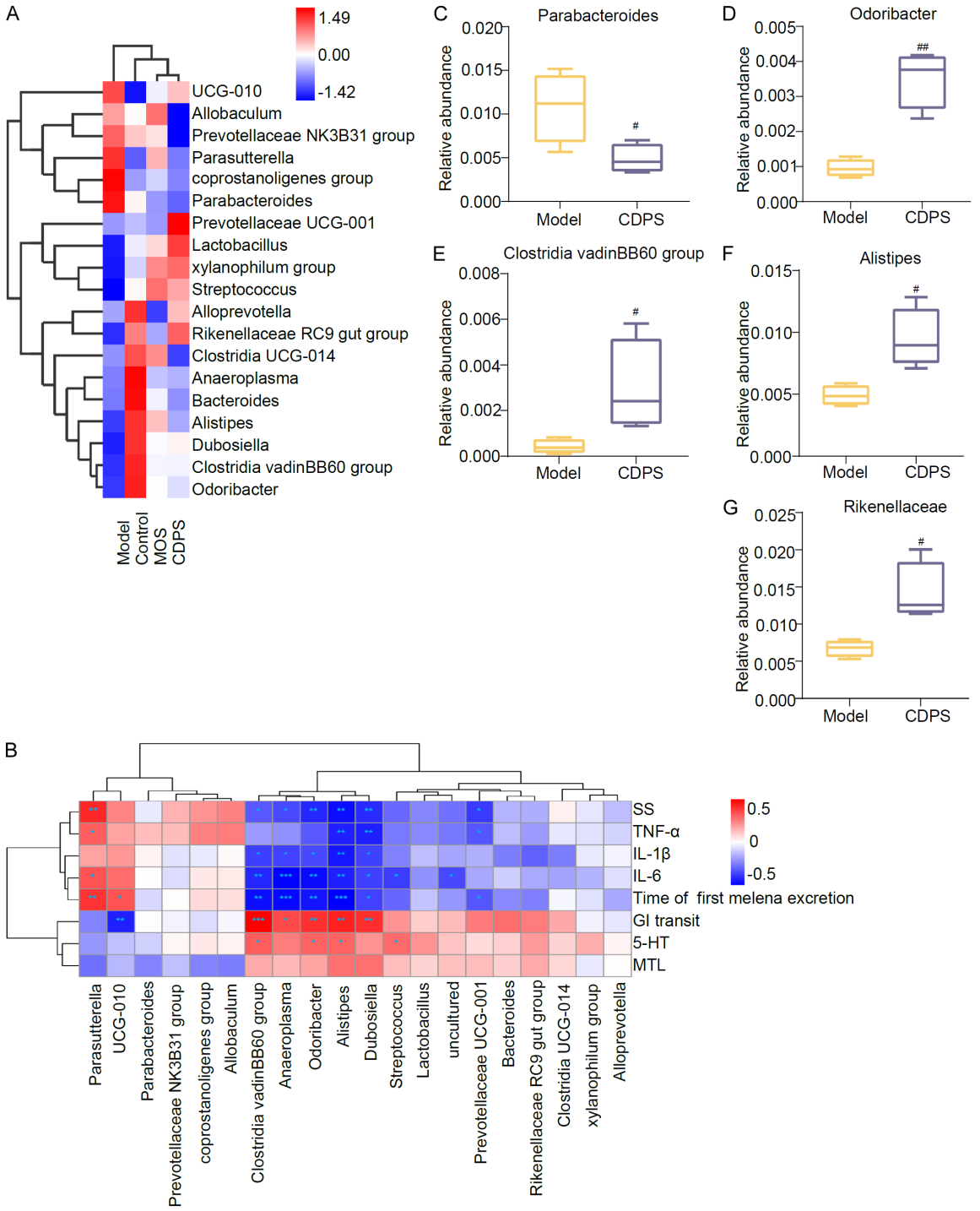

Figure 5. Characterization of gut microbiota of constipated mice. (A) Heat map with relative abundance of top 20 bacterial genera. (B) Correlation using Spearman rank correlation coefficient between 20 changed bacterial genera and constipation-related biomarkers. (C-G) Relative abundance of *Parabacteroides* (C), *Odoribacter* (D), *Clostridiales vadin BB60* group (E), *Alistipes* (F), and *Rikenellaceae* (G). Data are represented as mean ± SEM (n = 4). *P < 0.05, **P < 0.01, compared with the Control group; #P < 0.05, ##P < 0.01, compared with the Model group.

proliferation of interstitial cells of Cajal, which support peristalsis [33].

Linear discriminant analysis indicated that *Prevotellaceae UCG-001* was the most abun-

dant genus in the CDPS group (Figure S2A), suggesting its potential role as a CDPS target in managing constipation. *Prevotellaceae UCG-001* is a Gram-negative anaerobic bacterium known for producing SCFAs, such as acetic and butyric acids, by fermenting carbohydrates, which exerts anti-inflammatory effects and inhibits potential pathogens [34]. LEfSe (Linear discriminant analysis effect Size) analysis revealed that the *Proteobacteria* were most enriched in the Model group, identifying them as a likely contributor to constipation in mice (Figure S2B). Increased Proteobacteria abundance is associated with dysbiosis and epithelial dysfunction [35, 36]. In conclusion, these results demonstrate that CDPS mitigates constipation by modulating gut microbiota.

CDPS remodeled intestinal metabolites in constipated mice

The fecal samples of mice were analyzed to assess the gut metabolome profile using LC-MS, and 1153 metabolites were identified from patterns in negative and positive ion modes. Principal component and partial-least square discrimination analyses revealed a remarkable distinction between the Control and Model groups (**Figure 6A-C**). In addition, the CDPS and Control groups were highly similar in metabolite profiles, indicating that CDPS markedly modulates intestinal metabolites in constipated mice (**Figure 6D**). Volcano plots were used to identify differentially abundant metabolites based on a VIP score ≥ 1.0, Log|FC| > 1.5, and $P < 0.05$ (**Figure 6E**, **6F**). CDPS treatment significantly altered 262 metabolites, with 89 upregulated and 173 downregulated metabolites (**Figure 6G**). The differential metabolites were subjected to a KEGG enrichment analysis to determine the metabolic pathways associated with CDPS. The findings indicated that CDPS played a crucial role in alleviating constipation through several metabolic pathways such as primary bile acid biosynthesis, bile secretion, linoleic acid and others (**Figure 7A** and Table S3). The cluster heatmap results indicated noteworthy changes in metabolites such as linoleic acid, spermidine, prostaglandin H2, and LysoPC (17:0/0:0) following CDPS treatment (**Figure 7B**). LysoPC is known for its proinflammatory properties, increasing intestinal permeability, allowing potential pathogens to cross the intestinal barrier, and ultimately disrupting the mucosal integrity [37] (**Figure 7C-F**). Conversely, spermidine improves the gut barrier function by boosting the levels of tight junction proteins and mucins [38].

Analysis of constipation-associated microbiota and marker metabolites

Metabolites and bacteria associated with constipation were investigated using the Spearman rank analysis based on data from metabolome and microbiome analyses. Chenodeoxycholic acid showed a positive correlation with *Clostridiales vadin BB60* group, *Prevotellaceae UCG-001*, *Odoribacter*, and *Alistipes* while showing a negative correlation with *Parabacteroides*. Additionally, *Clostridiales vadin BB60* group was positively correlated with beneficial metabolites like spermidine and LysoPC (16:0/0:0), and negatively correlated with proinflammatory markers such as 6-keto-prostaglandin E1 and 20-carboxy-leukotriene B4 (**Figure 8**). These results suggest that CDPS relieves constipation in LOP-induced mice, possibly through interactions between gut microbes and metabolites.

Discussion

Constipation is a condition clinically characterized by slowed intestinal motility, dry and hard intestinal content, and prolonged retention. TCM and natural products offer a promising alternative to conventional constipation drugs, as they have fewer side effects. Among these natural products, polysaccharides have shown potential for influencing gut microbiota structure. Gut microbes are closely associated with the development of constipation, making it an important tool in the research of gastrointestinal diseases, with approaches like dominant microbiota modulation and fecal microbial transplantation emerging as important strategies for restoring intestinal homeostasis. The *Cistanche deserticola Ma* is a common TCM with defecating and intestine-moistening effects, with polysaccharides (CDPS) as one of its primary components [39]. Studies reported that CDPS can regulate intestinal flora and enhance immunocompetence [40, 41]. Dimidi et al. demonstrated that decoction of *Cistanche deserticola Ma* can significantly ameliorate small intestine movement and short defecation time in mice, with galactitol, a sugar alcohol, identified as an active ingredient contributing to these effects [40]. Yuan et al. investigated

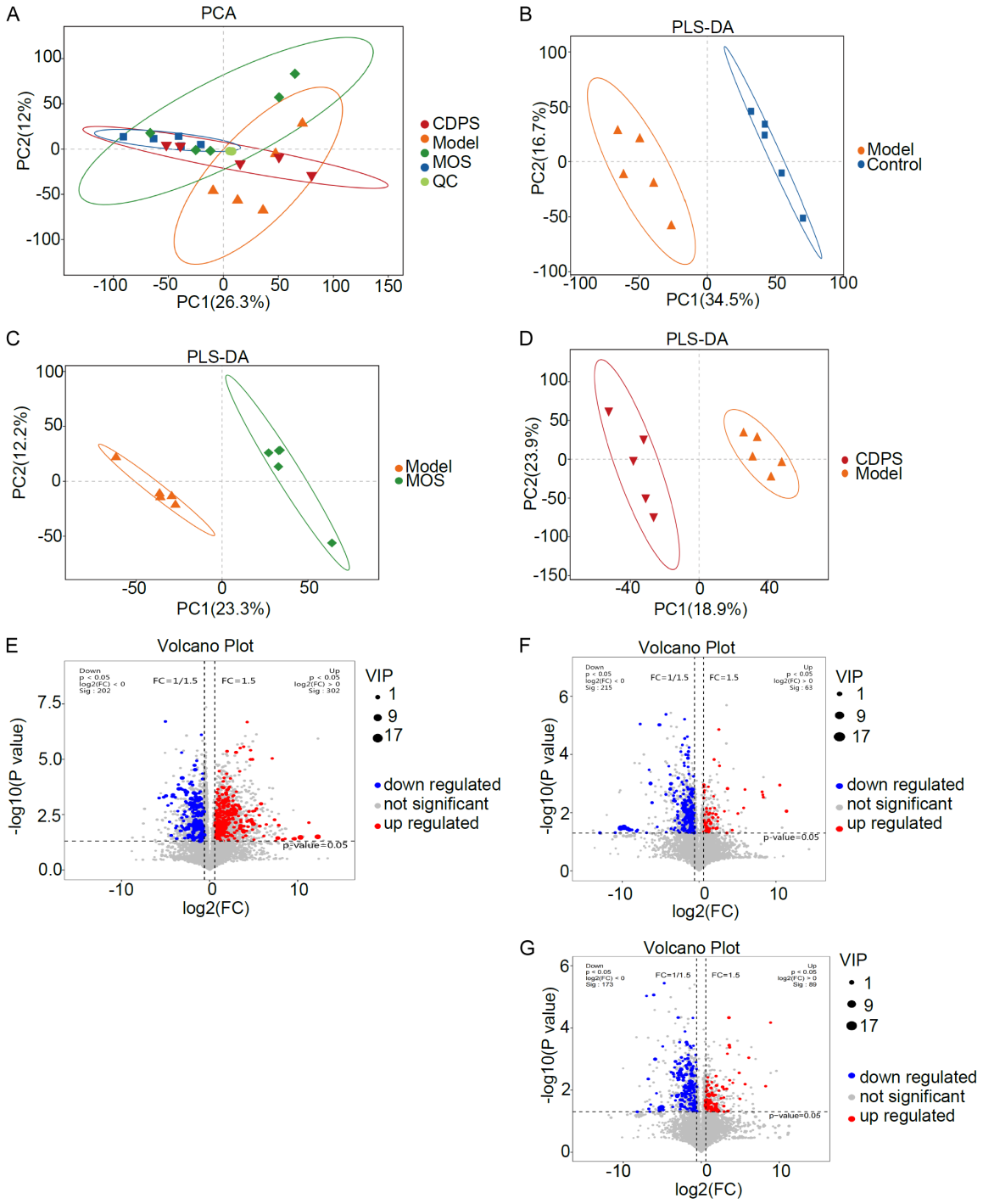

Figure 6. Metabolomic analysis of mouse fecal samples. (A) Principal component analysis (PCA) score plot. (B-D) Partial least square-discrimination analysis (PLS-DA) plot of Model and Control groups (B), MOS and Model groups (C), and CDPS and Model groups (D). (E-G) Volcano plot of Model and Control groups (E), MOS and Model groups (F), and CDPS and Model groups (G).

the effects of different varieties of *Cistanche deserticola Ma* for their constipation-relieving effects, reporting consistent laxative benefits across different varieties [41]. Evidence confirms that polysaccharides are key components of *Cistanche deserticola Ma*, which can accumulate in large quantities in the intestinal tract to exert laxative effects. In conclusion, these

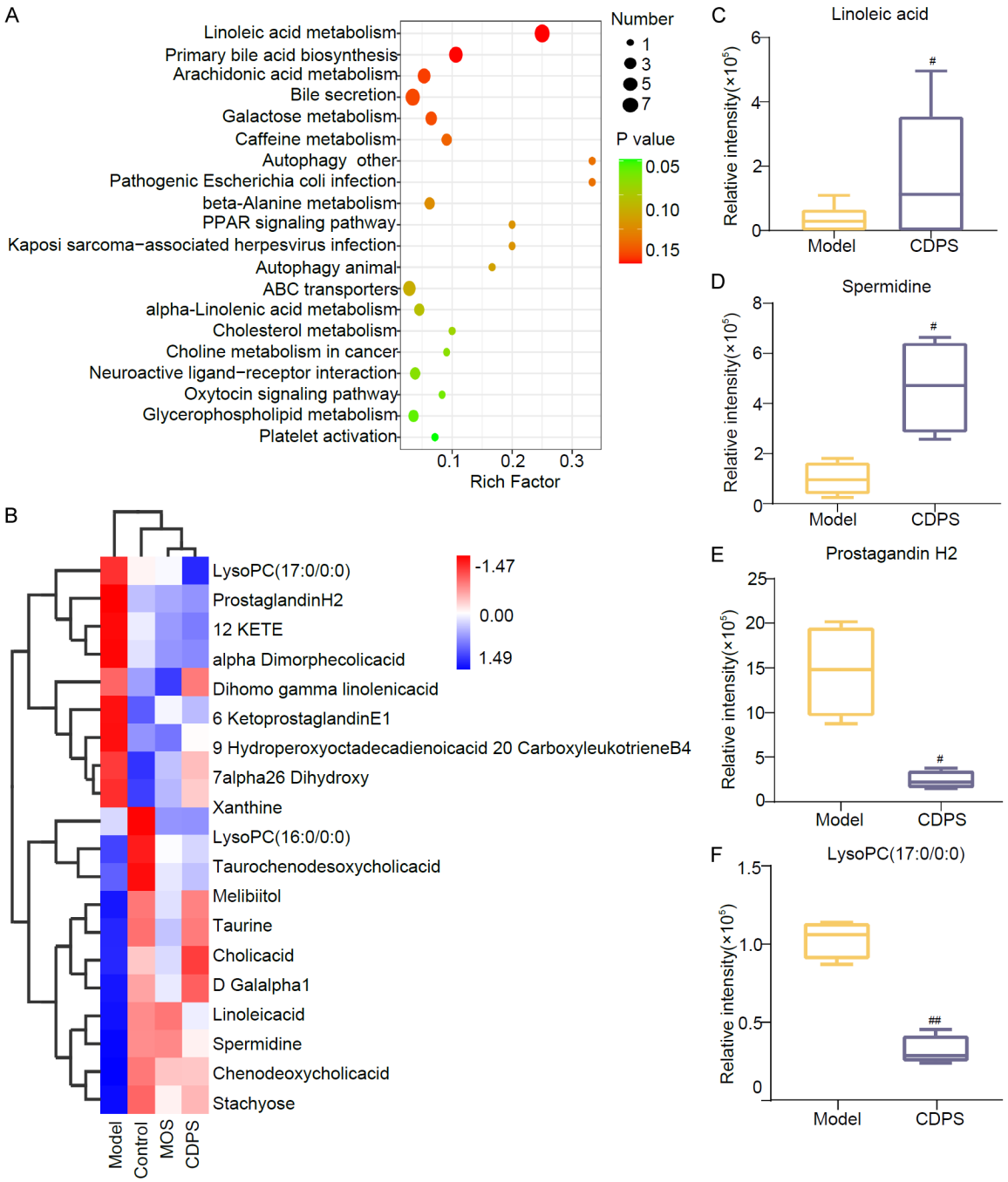

Figure 7. Pathway enrichment analysis of differential metabolites and marker metabolite clustering analysis. (A) Top 20 KEGG metabolic pathways associated with CDPS. (B) Clustering analysis with marker metabolites visualized as a heat map. (C-F) Relative intensity of linoleic acid (C), spermidine (D), prostaglandin H2 (E), and lysophosphatidylcholine (LysoPC) (17:0/0:0) (F). Data are represented as mean ± SEM (n = 4). *P < 0.05, **P < 0.01, compared with the Control group; #P < 0.05, ##P < 0.01, compared with the Model group.

studies support the laxative effect of *Cistanche deserticola Ma* as a promising natural remedy for constipation. However, the mechanisms of CDPS to ameliorate constipation is still not fully elucidated.

Recent studies indicate that CDPS may alleviate constipation by regulating oxidative stress and exerting neuroprotective effects via the Nrf2/Keap1 pathway [42]. Additional research suggests that this is closely related to the bile

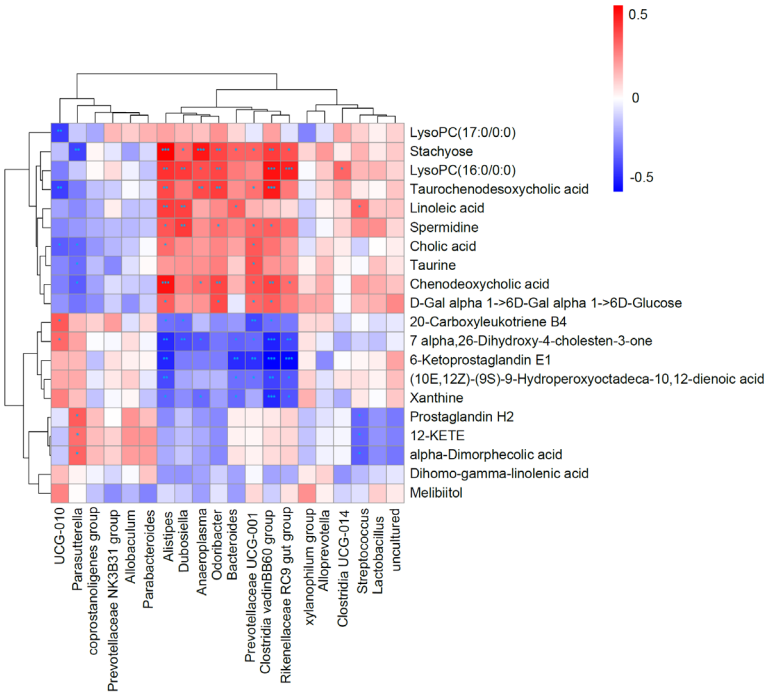

Figure 8. Correlation analysis between constipation-associated bacteria and marker metabolites.

acid metabolism pathway [43]. Remarkably, MAPK signaling pathway, especially the P38 and ERK isoforms, plays an essential role in the progression of constipation [44]. MAPK pathway can modify the molecular structure of tight junction complexes by regulating the expression of tight junction-associated proteins [45, 46]. Furthermore, several polysaccharides extracted from plants have been reported to regulate the MAPK pathway to protect the intestinal barrier and ameliorate constipation [47-49]. Based on these ideas, we speculated that CDPS might ameliorate constipation symptoms through regulating the MAPK pathway. Our findings confirmed that CDPS down-regulated proinflammatory factor levels by inhibiting the activation of MAPK pathway, specifically by down-regulating the phosphorylation of P38 and ERK (p-P38/P38 and p-ERK/ERK).

This study also demonstrates that CDPS upregulates serum levels of 5-HT and MTL while downregulating SS to relieve constipation. Intestinal hormones (e.g., MTL) and neurotransmitters (e.g., 5-HT, SS) play crucial roles in regulating gastrointestinal peristalsis [25]. Intestinal neurons of the human duodenum and colon express MTL receptors, which promote gastrointestinal motility, influence gastrointestinal digestion, and regulate small intestinal propulsion [50]. The neurotransmitter SS inhibits gastric acid secretion [51], whereas 5-HT, a neurotransmitter distributed in the gastrointestinal tract, links gut function with brain signaling. 5-HT is derived from gut microbial tryptophan [52], and lower levels are commonly found in the intestinal mucosa of constipation patients [53]. Enterochromaffin cells release 5-HT, which activates submucosal afferent nerve fibers and modulates local excitation and inhibition through the enteric nervous system [54]. Moreover, constipation is usually accompanied by intestinal mucosal injury and compromised intestinal barrier integrity. Tight junction complexes, which include transmembrane proteins such as OCLN and claudin (CLND) and cytoplasmic scaffold proteins such as ZO-1/2, connect to the actin cytoskeleton to form a continuous tight junction barrier within the intestinal epithelium [55]. Maintaining this barrier is crucial for resisting pathogenic bacteria and preventing local inflammatory infiltration [56]. In our study, CDPS promoted ZO-1 and OCLN expression to protect the integrity of the intestinal mucosal barrier. Besides, CDPS increased goblet cell number, restored small intestinal villi integrity, and reduced local inflammatory responses in constipated mice. In addition, CDPS restored mucus layer thickness to confer further protection to intestinal barrier function.

An imbalanced gut microbiota, marked by a decrease in beneficial bacteria and an increase in potentially harmful bacteria, is a decisive factor predisposing individuals to constipation [57]. In this study, 16S rRNA sequencing of fecal samples from mice was performed to analyze the gut microbiota structure, and results revealed that CDPS enhanced the abundance and diversity of the gut microbial community, restoring gut microbiota homeostasis in mice. Specifically, CDPS significantly increased the abundance of beneficial flora at the family level,

including *Lactobacillaceae* and *Rikenellaceae,* and at genus level, such as *Odoribacter*, *Clostridiales vadin BB60* group, and *Alistipes*.

Short-chain fatty acids (SCFAs) help maintain immune homeostasis in the intestinal environment and enhance mucosal barrier function by regulating tight junction complex structures [58]. In addition, some beneficial bacteria promote gastrointestinal motility by metabolizing organic acids such as SCFAs and bile acids [59]. We found that the abundance of bacteria involved in SCFA synthesis, *Lactobacillaceae*, *Rikenellaceae*, *Odoribacter, Alistipes*, and *Prevotellaceae UCG-001*, were significantly upregulated after CDPS treatment. Interestingly, these bacteria are all involved in butyric acid synthesis [29-34], a key energy source for intestinal energy cells that supports intestinal mucosal barrier integrity, regulates immune function, and reduces intestinal inflammation [61]. Our findings suggest that SCFAs may be one of the mechanisms of CDPS in treating constipation. LEfSe analysis revealed an enrichment of Proteobacteria in the Model group, identifying this phylum as a potentially pathogenic contributor to constipation in mice. Elevated Proteobacteria abundance disrupts intestinal mucosal barrier function, reduces intestinal mucus, increases permeability, and triggers low-grade inflammation [60-62]. In conclusion, these results overwhelmingly illustrate that CDPS alters gut microbiota structure and restores gut functional homeostasis.

Metabolomic study uncovered that CDPS significantly attenuated constipation in mice by modulating pathways related to primary bile acid biosynthesis, bile secretion, linoleic acid, with linoleic acid metabolism emerging as the most impactful pathway. Linoleic acid is an essential omega-6 fatty acid in the human body with crucial roles in regulating human immunity and reducing chronic intestinal inflammation [63]. This compound is involved in lipid and fatty acid metabolism, and certain intestinal bacteria such as *Lactobacillus*, *Lactococcus*, and *Bifidobacterium* metabolize linoleic acid [64]. Linoleic acid reduces inflammation by decreasing proinflammatory factors, such as TNF-α and IL-1, making it valuable for preventing and treating inflammatory bowel disease [65]. Arachidonic acid, a derivative of linoleic acid, is a polyunsaturated fatty acid whose metabolites (e.g., leukotrienes and prostaglandins) act as crucial inflammatory mediators in patients with ulcerative colitis [66]. These findings indicate that CDPS mitigates constipation in mice by regulating metabolic pathways such as linoleic and arachidonic acid pathways, among others.

There are still some shortcomings in this study: 1) Besides the MAPK pathway, future research should integrate transcriptomics to gain deeper insights into the mechanism by which CDPS alleviates constipation. 2) Further studies using germ-free animals and fecal microbiota transplants are recommended to confirm the role of gut microbiota and metabolites in constipation relief by CDPS and to better understand the interactions between gut microbiota and the host.

Conclusion

This study demonstrates that CDPS reduces the time to first melena excretion, modulates neurotransmitter and gastrointestinal hormone levels, enhances intestinal barrier integrity, and mitigates inflammatory responses. Furthermore, it offers novel insights into the mechanism of CDPS in alleviating constipation through fecal metabolomics and microbiomics. The findings indicate that CDPS enhances the function of the intestinal mucosal barrier and relieves constipation by regulating the gut microbiota structure and metabolites, increasing tight junction-related protein expression, inhibiting MAPK pathway activation, and downregulate proinflammatory factor.

Acknowledgements

This work was supported by the Jilin Scientific and Technological Development Program (20230204047YY).

Disclosure of conflict of interest

None.

Address correspondence to: Junpeng Guo, School of Clinical Medicine, Changchun University of Chinese Medicine, No. 1035 Boshuo Road, Changchun 130117, Jilin, China. Tel: +86-0431-81620335; E-mail: guojp1228@163.com

References

[1] Tanner S, Chaudhry A, Goraya N, Badlani R, Jehangir A, Shahsavari D, Malik Z and Parkman

HP. Prevalence and clinical characteristics of dyssynergic defecation and slow transit constipation in patients with chronic constipation. J Clin Med 2021; 10: 2027.
[2] Bharucha AE and Lacy BE. Mechanisms, evaluation, and management of chronic constipation. Gastroenterology 2020; 158: 1232-1249.e3.
[3] Bassotti G, Gambaccini D and Bellini M. Prucalopride succinate for the treatment of constipation: an update. Expert Rev Gastroenterol Hepatol 2016; 10: 291-300.
[4] Włodarczyk J, Waśniewska A, Fichna J, Dziki A, Dziki Ł and Włodarczyk M. Current overview on clinical management of chronic constipation. J Clin Med 2021; 10: 1738.
[5] Ding C, Ge X, Zhang X, Tian H, Wang H, Gu L, Gong J, Zhu W and Li N. Efficacy of synbiotics in patients with slow transit constipation: a prospective randomized trial. Nutrients 2016; 8: 605.
[6] Li R, Li M, Li B, Chen WH and Liu Z. Cannabis sativa L. alleviates loperamide-induced constipation by modulating the composition of gut microbiota in mice. Front Pharmacol 2022; 13: 1033069.
[7] Henao-Mejia J, Elinav E, Thaiss CA, Licona-Limon P and Flavell RA. Role of the intestinal microbiome in liver disease. J Autoimmun 2013; 46: 66-73.
[8] Tremaroli V and Bäckhed F. Functional interactions between the gut microbiota and host metabolism. Nature 2012; 489: 242-249.
[9] Obata Y and Pachnis V. The effect of microbiota and the immune system on the development and organization of the enteric nervous system. Gastroenterology 2016; 151: 836-844.
[10] Mayer EA, Savidge T and Shulman RJ. Brain-gut microbiome interactions and functional bowel disorders. Gastroenterology 2014; 146: 1500-1512.
[11] Li Y, Long S, Liu Q, Ma H, Li J, Xiaoqing W, Yuan J, Li M and Hou B. Gut microbiota is involved in the alleviation of loperamide-induced constipation by honey supplementation in mice. Food Sci Nutr 2020; 8: 4388-4398.
[12] He Q, Han C, Huang L, Yang H, Hu J, Chen H, Dou R, Ren D and Lin H. Astragaloside IV alleviates mouse slow transit constipation by modulating gut microbiota profile and promoting butyric acid generation. J Cell Mol Med 2020; 24: 9349-9361.
[13] Zhang X, Yang H, Zheng J, Jiang N, Sun G, Bao X, Lin A and Liu H. Chitosan oligosaccharides attenuate loperamide-induced constipation through regulation of gut microbiota in mice. Carbohydr Polym 2021; 253: 117218.
[14] Zhou S, Feng D, Zhou Y, Duan H, Jiang Y and Yan W. Analysis of the active ingredients and health applications of cistanche. Front Nutr 2023; 10: 1101182.
[15] Cheng N, Wang H, Hao H, Rahman FU and Zhang Y. Research progress on polysaccharide components of Cistanche deserticola as potential pharmaceutical agents. Eur J Med Chem 2023; 245: 114892.
[16] Fu Z, Fan X, Wang X and Gao X. Cistanches Herba: an overview of its chemistry, pharmacology, and pharmacokinetics property. J Ethnopharmacol 2018; 219: 233-247.
[17] Kumar V, Sinha AK, Makkar HP, de Boeck G and Becker K. Dietary roles of non-starch polysaccharides in human nutrition: a review. Crit Rev Food Sci Nutr 2012; 52: 899-935.
[18] Ma H, Xiong H, Zhu X, Ji C, Xue J, Li R, Ge B and Cui H. Polysaccharide from Spirulina platensis ameliorates diphenoxylate-induced constipation symptoms in mice. Int J Biol Macromol 2019; 133: 1090-1101.
[19] Liu X, Jian C, Li M, Wei F, Liu H and Qin X. Microbiome-metabolomics deciphers the effects of Cistanche deserticola polysaccharides on aged constipated rats. Food Funct 2022; 13: 3993-4008.
[20] Percie du Sert N, Hurst V, Ahluwalia A, Alam S, Avey MT, Baker M, Browne WJ, Clark A, Cuthill IC, Dirnagl U, Emerson M, Garner P, Holgate ST, Howells DW, Karp NA, Lazic SE, Lidster K, MacCallum CJ, Macleod M, Pearl EJ, Petersen OH, Rawle F, Reynolds P, Rooney K, Sena ES, Silberberg SD, Steckler T and Würbel H. The ARRIVE guidelines 2.0: updated guidelines for reporting animal research. PLoS Biol 2020; 18: e3000410.
[21] Chen Y, Zhang R, Xu J and Ren Q. Alteration of intestinal microflora by the intake of millet porridge improves gastrointestinal motility. Front Nutr 2022; 9: 965687.
[22] Huang J, Lin B, Zhang Y, Xie Z, Zheng Y, Wang Q and Xiao H. Bamboo shavings derived O-acetylated xylan alleviates loperamide-induced constipation in mice. Carbohydr Polym 2022; 276: 118761.
[23] Satish SR, Noriaki M, Yusuke K, Y, Kazutaka N, Atsushi N and Shin F. Comparative profiles of lubiprostone, linaclotide, and elobixibat for chronic constipation: a systematic literature review with meta-analysis and number needed to treat/harm. BMC Gastroenterol 2024; 24: 12.
[24] Chen L, Zhang J, Suo H, Wang W, Wang H, Zhang Y, Hu Q, Zhao X and Li J. Preventive effects of different fermentation times of shuidouchi on diphenoxylate-induced constipation in mice. Foods 2019; 8: 86.
[25] Wang L, Chen C, Cui S, Lee YK, Wang G, Zhao J, Zhang H and Chen W. Adhesive bifidobacterium induced changes in cecal microbiome alleviated constipation in mice. Front Microbiol 2019; 10: 1721.

[26] Pu J, Chen D, Tian G, He J, Huang Z, Zheng P, Mao X, Yu J, Luo J, Luo Y, Yan H and Yu B. All-trans retinoic acid attenuates transmissible gastroenteritis virus-induced inflammation in IPEC-J2 cells via suppressing the RLRs/NF-κB signaling pathway. Front Immunol 2022; 13: 734171.

[27] Marin DE, Motiu M and Taranu I. Food contaminant zearalenone and its metabolites affect cytokine synthesis and intestinal epithelial integrity of porcine cells. Toxins (Basel) 2015; 7: 1979-88.

[28] Taranu I, Marin DE, Braicu C, Pistol GC, Sorescu I, Pruteanu LL, Berindan Neagoe I and Vondnar DC. In vitro transcriptome response to a mixture of lactobacilli strains in intestinal porcine epithelial cell line. Int J Mol Sci 2018; 19: 1923.

[29] Li S, He Y, Zhang H, Zheng R, Xu R, Liu Q, Tang S, Ke X and Huang M. Formulation of traditional Chinese medicine and its application on intestinal flora of constipated rats. Microb Cell Fact 2020; 19: 212.

[30] Morgan XC, Tickle TL, Sokol H, Gevers D, Devaney KL, Ward DV, Reyes JA, Shah SA, LeLeiko N, Snapper SB, Bousvaros A, Korzenik J, Sands BE, Xavier RJ and Huttenhower C. Dysfunction of the intestinal microbiome in inflammatory bowel disease and treatment. Genome Biol 2012; 13: R79.

[31] Labus JS, Osadchiy V, Hsiao EY, Tap J, Derrien M, Gupta A, Tillisch K, Le Neve B, Grinsvall C, Ljungberg M, Ohman L, Tornblom H, Simren M and Mayer EA. Evidence for an association of gut microbial Clostridia with brain functional connectivity and gastrointestinal sensorimotor function in patients with irritable bowel syndrome, based on tripartite network analysis. Microbiome 2019; 7: 45.

[32] Wada Y, Nishiyama M, Uehara H, Sato K, Hamamoto Y, Ogihara H, Nishi A, Asakawa T and Yamamoto M. Microbiome biomarkers associated with the gut contraction response elicited by the Japanese traditional medicine daikenchuto. Gene 2022; 826: 146262.

[33] Yao Z, Fu S, Ren B, Ma L and Sun D. Based on network pharmacology and gut microbiota analysis to investigate the mechanism of the laxative effect of pterostilbene on loperamide-induced slow transit constipation in mice. Front Pharmacol 2022; 13: 913420.

[34] Zou J, Shen Y, Chen M, Zhang Z, Xiao S, Liu C, Wan Y, Yang L, Jiang S, Shang E, Qian D and Duan J. Lizhong decoction ameliorates ulcerative colitis in mice via modulating gut microbiota and its metabolites. Appl Microbiol Biotechnol 2020; 104: 5999-6012.

[35] Hrncirova L, Machova V, Trckova E, Krejsek J and Hrncir T. Food preservatives induce proteobacteria dysbiosis in human-microbiota associated Nod2-deficient mice. Microorganisms 2019; 7: 383.

[36] Litvak Y, Byndloss MX, Tsolis RM and Bäumler AJ. Dysbiotic Proteobacteria expansion: a microbial signature of epithelial dysfunction. Curr Opin Microbiol 2017; 39: 1-6.

[37] Wang L, Tao JH, Chen YF, Shen YM and Jiang S. Lizhong decoction ameliorates ulcerative colitis in mice via regulation of plasma and urine metabolic profiling. Chin J Integr Med 2022; 28: 1015-1022.

[38] Ma L, Ni Y, Wang Z, Tu W, Ni L, Zhuge F, Zheng A, Hu L, Zhao Y, Zheng L and Fu Z. Spermidine improves gut barrier integrity and gut microbiota function in diet-induced obese mice. Gut Microbes 2020; 12: 1-19.

[39] Kong ZL, Johnson A, Ko FC, He JL and Cheng SC. Effect of cistanche tubulosa extracts on male reproductive function in streptozotocin-nicotinamide-induced diabetic rats. Nutrients 2018; 10: 1562.

[40] Dimidi E, Christodoulides S, Scott SM and Whelan K. Mechanisms of action of probiotics and the gastrointestinal microbiota on gut motility and constipation. Adv Nutr 2017; 8: 484-494.

[41] Gao Y, Li B, Liu H, Tian Y, Gu C, Du X, Bu R, Gao J, Liu Y and Li G. Cistanche deserticola polysaccharides alleviate cognitive decline in aging model mice by restoring the gut microbiota-brain axis. Aging (Albany NY) 2021; 13: 15320-15335.

[42] Jiang HY, Ma RA, Ji FL, Liu Y, Wang B, Fu SQ, Ma LS, Wang S, Liu CX, Guo Z, Li R, Wang YC, Sun W, Dong L, Dong CX and Sun DQ. Structure characterization of polysaccharides from Cistanche deserticola and their neuroprotective effects against oxidative stress in slow transit constipation mice. Int J Biol Macromol 2024; 260: 129527.

[43] Yin H, Gao X, Yang H, Xu Z, Wang X, Wang X, Gao Y, Shi Z, Chen X, Cao L, Zhang C, Wang Z, Hu H and Xiao W. Total alditols from Cistanche deserticola attenuate functional constipation by regulating bile acid metabolism. J Ethnopharmacol 2024; 320: 117420.

[44] Li S, Shi Y, Zhu J, Li J, Wang S and Liu C. Protective effect of oxytocin on vincristine-induced gastrointestinal dysmotility in mice. Front Pharmacol 2024; 15: 1270612.

[45] Tak LJ, Kim HY, Ham WK, Agrahari G, Seo Y, Yang JW, An EJ, Bang CH, Lee MJ, Kim HS and Kim TY. Superoxide dismutase 3-transduced mesenchymal stem cells preserve epithelial tight junction barrier in murine colitis and attenuate inflammatory damage in epithelial organoids. Int J Mol Sci 2021; 22: 6431.

[46] Zhang X, Zheng J, Jiang N, Sun G, Bao X, Kong M, Cheng X, Lin A and Liu H. Modulation of gut microbiota and intestinal metabolites by lactulose improves loperamide-induced constipation in mice. Eur J Pharm Sci 2021; 158: 105676.
[47] Song J, Zhao X, Bo J, Lv Z, Li G, Chen Y, Liang J, Zhang C, Jin X, Liu C and Chang J. A polysaccharide from Alhagi honey protects the intestinal barrier and regulates the Nrf2/HO-1-TLR4/MAPK signaling pathway to treat alcoholic liver disease in mice. J Ethnopharmacol 2024; 321: 117552.
[48] Cheng X, Zhu Y, Huang J, Li Y, Jiang X and Yang Q. A neutral polysaccharide from Persicaria hydropiper (L.) Spach ameliorates lipopolysaccharide-induced intestinal barrier injury via regulating the gut microbiota and modulating AKT/PI3K/mTOR and MAPK signaling pathways. J Ethnopharmacol 2024; 320: 117403.
[49] Feng Y, Chen S, Song Y, Liu S, Duan Y, Cai M, Kong T and Zhang H. A novel Sagittaria sagittifolia L. polysaccharides mitigate DSS-induced colitis via modulation of gut microbiota and MAPK/NF-κB signaling pathways. Int J Biol Macromol 2024; 254: 127835.
[50] Zhang ZH, Wu SD, Wang B, Su Y, Jin JZ, Kong J and Wang HL. Sphincter of Oddi hypomotility and its relationship with duodenal-biliary reflux, plasma motilin and serum gastrin. World J Gastroenterol 2008; 14: 4077-4081.
[51] Suo H, Zhao X, Qian Y, Sun P, Zhu K, Li J and Sun B. Lactobacillus fermentum suo attenuates HCl/ethanol induced gastric injury in mice through its antioxidant effects. Nutrients 2016; 8: 155.
[52] Rosser EC, Piper CJM, Matei DE, Blair PA, Rendeiro AF, Orford M, Alber DG, Krausgruber T, Catalan D, Klein N, Manson JJ, Drozdov I, Bock C, Wedderburn LR, Eaton S and Mauri C. Microbiota-derived metabolites suppress arthritis by amplifying aryl-hydrocarbon receptor activation in regulatory B cells. Cell Metab 2020; 31: 837-851, e10.
[53] Miwa J, Echizen H, Matsueda K and Umeda N. Patients with constipation-predominant irritable bowel syndrome (IBS) may have elevated serotonin concentrations in colonic mucosa as compared with diarrhea-predominant patients and subjects with normal bowel habits. Digestion 2001; 63: 188-94.
[54] Cao YN, Feng LJ, Wang BM, Jiang K, Li S, Xu X, Wang WQ, Zhao JW and Wang YM. Lactobacillus acidophilus and Bifidobacterium longum supernatants upregulate the serotonin transporter expression in intestinal epithelial cells. Saudi J Gastroenterol 2018; 24: 59-66.
[55] Kaminsky LW, Al-Sadi R and Ma TY. IL-1beta and the intestinal epithelial tight junction barrier. Front Immunol 2021; 12: 767456.
[56] Zhou X, Liu X, He Q, Wang M, Lu H, You Y, Chen L, Cheng J, Li F, Fu X, Kwan HY, Zhou L and Zhao X. Ginger extract decreases susceptibility to dextran sulfate sodium-induced colitis in mice following early antibiotic exposure. Front Med (Lausanne) 2022; 8: 755969.
[57] Fu R, Li Z, Zhou R, Li C, Shao S and Li J. The mechanism of intestinal flora dysregulation mediated by intestinal bacterial biofilm to induce constipation. Bioengineered 2021; 12: 6484-6498.
[58] Xie Y, Wang C, Zhao D, Zhou G and Li C. Processing method altered mouse intestinal morphology and microbial composition by affecting digestion of meat proteins. Front Microbiol 2020; 11: 511.
[59] Yi R, Zhou X, Liu T, Xue R and Yang Z. Amelioration effect of Lactobacillus plantarum KFY02 on low-fiber diet-induced constipation in mice by regulating gut microbiota. Front Nutr 2022; 9: 938869.
[60] Heinritz SN, Weiss E, Eklund M, Aumiller T, Heyer CM, Messner S, Rings A, Louis S, Bischoff SC and Mosenthin R. Impact of a high-fat or high-fiber diet on intestinal microbiota and metabolic markers in a pig model. Nutrients 2016; 8: 317.
[61] Shin NR, Whon TW and Bae JW. Proteobacteria: microbial signature of dysbiosis in gut microbiota. Trends Biotechnol 2015; 33: 496-503.
[62] Gu X, Zhang S, Ma W, Wang Q, Li Y, Xia C, Xu Y, Zhang T, Yang L and Zhou M. The impact of instant coffee and decaffeinated coffee on the gut microbiota and depression-like behaviors of sleep-deprived rats. Front Microbiol 2022; 13: 778512.
[63] Men Y, Fu S, Xu C, Zhu Y and Sun Y. Supercritical fluid CO2 extraction and microcapsule preparation of Lycium barbarum residue oil rich in zeaxanthin dipalmitate. Foods 2021; 10: 1468.
[64] Helmy YA, Kathayat D, Deblais L, Srivastava V, Closs G Jr, Tokarski RJ 2nd, Ayinde O, Fuchs JR and Rajashekara G. Evaluation of novel quorum sensing inhibitors targeting auto-inducer 2 (AI-2) for the control of avian pathogenic escherichia coli infections in chickens. Microbiol Spectr 2022; 10: e0028622.
[65] Zhou B, Liu J, Wang Y, Wu F, Wang C, Wang C, Liu J and Li P. Protective effect of ethyl rosmarinate against ulcerative colitis in mice based on untargeted metabolomics. Int J Mol Sci 2022; 23: 1256.
[66] Burrello C, Giuffrè MR, Macandog AD, Diaz-Basabe A, Cribiu FM, Lopez G, Borgo F, Nezi L, Caprioli F, Vecchi M and Facciotti F. Fecal microbiota transplantation controls murine chronic intestinal inflammation by modulating immune cell functions and gut microbiota composition. Cells 2019; 8: 517.

Table S1. Mass spectrometry parameters

Parameter	Positive ions	Negative ions
Spray Voltage (V)	3800	-3000
Sheath Gas Flow Rate (Arb)	35	35
S-lens RF level	50	50
NCE/stepped NCE	10, 20, 40	10, 20, 40
MS/MS resolution	17500	17500
Mass range (m/z)	100-1200	100-1200
Full ms resolution	70000	70000
Capillary Temperature (°C)	320	320
Aux gas heater temperature (°C)	350	350
Aux gas flow rate (Arb)	8	8

MS: mass spectrum; NCE: normalized collision energies.

Table S2. Elution gradient

Time	A%	B%
0	95	5
10	20	80
14	0	100
16	95	5

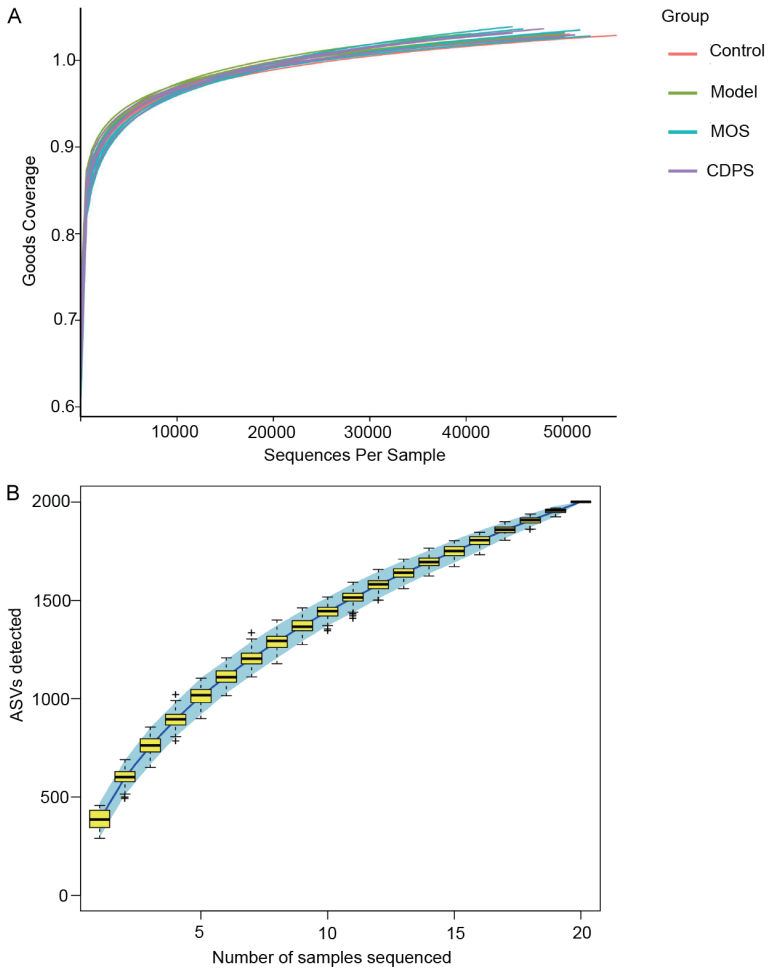

Figure S1. Species numbers and sequencing depth profiles. A. Goods coverage. B. Number of sequenced.

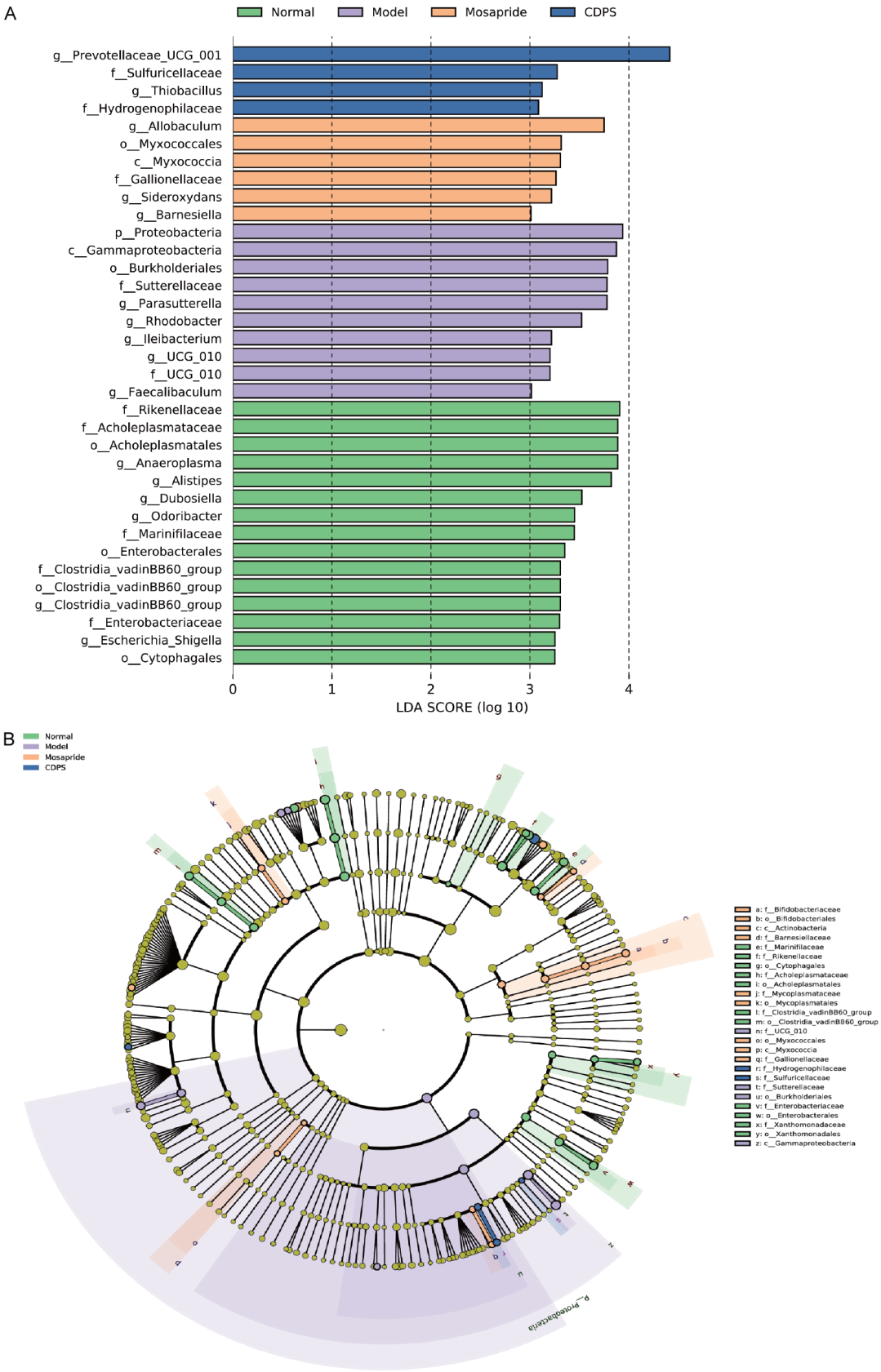

Figure S2. Identification of most characteristic taxa among experimental groups by linear discriminant analysis (LDA) effect size (LEfSe). A. Most significant differences of intestinal bacteria taxa among four groups after LDA using a threshold score larger than 3.0. B. Taxonomic abundance analysis on differentially enriched taxa among four groups using LEfSe.

Table S3. KEGG pathway enrichment

No.	Pathway	Hits	*P*_value	Impact	Metabolites
1	Linoleic acid metabolism	7	1.76E-08	0.25	(10E,12Z)-(9S)-9-Hydroperoxyoctadeca-10,12-dienoic acid, 7S,8S-DiHODE, 9,10-DHOME, 9,10-epoxy-13-hydroxy-11-octadecenoic acid, alpha-Dimorphecolic acid, Dihomo-gamma-linolenic acid, Linoleic acid
2	Primary bile acid biosynthesis	5	0.000183884	0.1	7 alpha,26-Dihydroxy-4-cholesten-3-one, Chenodeoxycholic acid, Cholic acid, Taurine, Taurochenodesoxycholic acid
3	Arachidonic acid metabolism	4	0.010835826	0.05	12-KETE, 20-Carboxyleukotriene B4, 6-Ketoprostaglandin E1, Prostaglandin H2
4	Bile secretion	6	0.014635815	0.03	Aspirin, Pregnanediol-3-glucuronide, Benzoyl glucuronide (Benzoic acid), Spermidine, Chenodeoxycholic acid, Cholic acid
5	Galactose metabolism	3	0.016006095	0.06	D-Gal alpha 1→6D-Gal alpha 1→6D-Glucose, Melibiitol, Stachyose
6	Caffeine metabolism	2	0.026702791	0.09	Theobromine, Xanthine

Significantly enriched pathways: Hit ≥ 2, P < 0.05.